ELSEVIER

Cement & Concrete Composites 23 (2001) 189–200

Cement & Concrete Composites

www.elsevier.com/locate/cemconcomp

Reconstructions by SPACE of the Interfacial Transition Zone

Piet Stroeven [a,*], Martijn Stroeven [b]

[a] *Faculty of Civil Engineering and Geosciences, Delft University of Technology, Stevinweg 4, 2628 Delft, The Netherlands*
[b] *HABANERA, Delft, The Netherlands*

Abstract

Of particular interest in concrete technology is the so-called Interfacial Transition Zone (ITZ). Conflicting experimental evidences as to the internal structure and extent of the ITZ, and even as to the very existence of it, make it attractive to confront such observations with a coherent picture of the ITZ produced by computer-simulation, although based on a simplified model concept. This contribution outlines the scientific framework for interpretation of the so-called packing phenomenon. A dynamic computer-simulation system, Software Package for the Assessment of Compositional Evolution, with the acronym SPACE was recently developed by the second author, and has been used for the present purpose. In addition to properly simulating composition of particulate materials, as can also be achieved by conventional systems based on random sequential procedures, it has been demonstrated earlier that SPACE can also more accurately reproduce configuration of particles in such materials. An hydration algorithm is additionally implemented in SPACE. Some preliminary information on gradient structures in the ITZ are discussed. The extent of packing gradients in the fresh and hardened state will be shown to vary with changes in material composition (water to cement ratio, cement fineness) and in the configuration-sensitivity of the parameter being studied. This implies structural gradients to extend further away from aggregate grain surfaces the more sensitive the very parameter is to packing configuration. Particular emphasis is given to this fundamental aspect, and not to properly estimating the ITZ's thickness of this model cement paste near boundaries. Tools are provided to extract 2-D structural data from imaginary section planes (or from imaginary thin section projections) of the ITZ parallel to the interface. By making use of stereological methods, such data are given a 3-D structural meaning. Of course, direct information on porosity, packing characteristics and local particle distributions is available in 3-D. Therefore, in some cases direct 3-D measurements are possible, as well as visualisation of parts of the structure. © 2001 Published by Elsevier Science Ltd.

Keywords: Composition; Configuration; Hydration; Interfacial transition zone; Material model; Particle packing; Stereology; Structure-sensitivity

1. Introduction

Popular methods which are used today for modelling material characteristics are continuum-based numerical approaches, like the finite-element method, allowing to predict the behaviour of a material under various conditions. These methods are based on the assumption that the internal structure of the material can be considered continuous. Some materials, however, clearly display a discontinuous internal structure, of which the behaviour is strongly influenced by their granularity. The uniformity of the packing of powders in the production process of ceramics, for example, significantly influences the performance of the material. Crack development in concrete is another example of a phenomenon depending on the 'group behaviour' [1] of the aggregate particles on meso-level and the packing details of the binder particles on micro-level.

Cementitious materials can be considered consisting of particulate elements on the various levels of the microstructure. In an ordered fashion, they build up crystalline structure in the hydrated state. The binder particles in fresh concrete form on microlevel the so-called matrix. When matured, the matrix stabilises the skeleton of aggregate particle on meso-level. To realistically simulate this densely packed particulate matter, the common simulation methods based on sequential random-generator procedures are unsuitable. More specifically, they are *unpractical* due to the excessive computer time requirements at high particle densities, and they are *unreliable*, because the rejection proce-

* Corresponding author. Tel.: +31-015-278-4035; fax: +31-015-261-1465.
E-mail address: p.stroeven@ct.tudelft.nl (P. Stroeven).

0958-9465/01/$ - see front matter © 2001 Published by Elsevier Science Ltd.
PII: S0958-9465(00)00076-7

dure leads to biases in particle configuration that are dramatically increasing with particle density [2]. This adds to the obscurity in comparing various experimental and computer-simulation data. To approach reality more closely, the Software Package for the Assessment of Compositional Evolution (SPACE) system has been developed, and recently introduced in the international literature [3]. The SPACE system is based on a dynamic concept of simulating the production process of composite materials. For a description of the *details* of the generation system, see [2,3]. This paper will only mention the conceptual elements in the set up of this system. It will be applied in this paper to illustrate the dependence of the extent of the Interfacial Transition Zone (ITZ) on the structure-sensitivity of the material parameter at issue.

The paramount interest in the ITZ in cementitious composites is derived from the recognition that in normal concretes the ITZ constitutes the weakest link in the mechanical system. Hence, methods for upgrading concrete into the high strength or even high performance ranges should be in the first place effective in disproportional improving the 'quality' of the ITZ [4]. In doing so, the impact of the ITZ on material performance can be completely eliminated, leading to high strength and also to extreme brittleness. A significant reduction in the water to cement ratio, rendered possible by the use of superplasticizer, has been demonstrated as a method for achieving this goal. Increasing the range of particle sizes in the binder by adding fine-ground fly ash or rice-husk ash, also works out favourably [5]. The underlying particle packing mechanism is strongly reinforced by adding the much finer silica fume, leading to DSP (Densified with Small Particles) concrete. Almost the same mechanical effects were obtained by replacing these pozzolanic particles by inert ones of similar fineness (i.e. of carbon black [6]). Hence, physical binding forces of Van der Waals type, that are relying on the pattern of inter-particle distances, provide an important contribution to material strength.

Since reality is inherently complex, the ITZ is commonly physically modelled around aggregate grains as a shell-like zone with a certain thickness [7,8]. Segdregation in the cement particle packing near a surface (of aggregate grain or reinforcement bar), is commonly expressed in terms of density or porosity data. This is a measure for structural *composition*. We deal here in relative terms with 'how much of a certain phase', hence, with volume fraction of a material phase (that could be void). When obtained by high-resolution methods like (electron) microscopy or X-ray diffraction, a relatively thin interface layer is found (say, 20–40 μm). A low-resolution approach to detecting composition gradients is by micro-hardness measurements [9]. The averaging effect of the indenter head inevitably leads to a more extended interface layer, of, say, 100 μm. A gradient in porosity (or density) in the interphase zone is the direct consequence of uneven cement particle packing. The amount of unhydrated cement after hydration, however, depends on size segregation and on the distance distribution of particles (availability of water during hydrating!). Hence, here we deal with a *configuration* parameter of the fresh cement paste, where group behaviour is essential. Configuration deals with the spatial arrangement of particles in a group. Like in case of composition, configuration homogeneity is defined in statistical terms. The associated representative volume element will contain with, say, 99% probability a 'representative' set of mutual grain positions [10]. As we will see later, configuration homogeneity will be achieved much further away from the interface surface than composition homogeneity, confirming similar experimental findings [7]. This contribution will particularly focus on this fundamental aspect of particle packing. Because of its scale-invariance, it holds for the meso-level (aggregate packing near exterior surfaces), as well as for the micro-level (binder particles in the fresh state of 'the' ITZ).

In trying to fit seemingly conflicting experimental results into a materials science framework, we have to recognise that such results are also influenced by the sampling strategy. When interested in the extent of the ITZ around aggregate particles in concrete, a specimen is cast and sectioned, displaying the ITZ around *particle sections* of various sizes. Of course, the size of an arbitrary particle section cannot be related in a direct way to the real size of the aggregate particle. A rough idea can only be obtained (after completion of the ITZ study) by 3-D reconstruction, i.e., by using the two parts of the same particle that was cut by the sawing machine. As a result, mostly, observations will be biased to an unknown degree. Even a 'random set' of particle sections has been demonstrated by Stroeven [11] to yield estimates for the thickness of the ITZ which are on average about 50% too high. Of course, specifically for this purpose prepared interphase areas will not necessarily represent actual 3-D conditions in real materials. For an excellent survey of the methodological aspects of studying the ITZ, see Scrivener [12].

2. Numerical modelling

The non-homogeneous, or granular, nature of the internal material structure is represented by a set of *distinct elements*. Each element corresponds to a distinguishable, characteristic phase in the material. For example, concrete is modelled as a set of elements representing the aggregate particles. The elements are

dispersed in a presumably homogeneous mortar matrix moulded in a container. Similarly, cement paste is modelled as a set of elements representing cement particles dispersed in water. The parameters describing the static conditions of the internal structure are the locations, orientations, and shapes of the various individual elements. Since the elements represent real physical phases in the material, physical properties can be assigned to each element along with its shape and size, at least *in principle*. The most difficult task, however, is the derivation of the location and the orientation of these non-overlapping elements.

2.1. Static simulation of particle positions

In a static simulation system, the particles will be sequentially located inside a container. Each location is governed by randomly generated co-ordinates. 'Overlap' with earlier generated particles will result in rejection, whereupon the generation process is continued. The number of rejections will increase dramatically at high volume fractions, making the generation process very time-consuming, if not impossible at all in the highest density range. Simulation of a multi-size particle composite requires starting with the largest particles in the mix. The system obviously excludes the mechanism of *mutual particle interaction*, which is so characteristic for the production stage of cementitious materials. The re-generation after rejection inevitably leads to an under-estimation of a natural phenomenon as particle clustering [13]. The generated nearest neighbour distribution of the particles will reveal, as a consequence, dramatically large biases at higher particle densities [13]. Three of the more popular systems in this category were developed by Roelfstra [14], by Diekkämper [15], and at NIST [16].

2.2. Dynamic simulation of particle positions

The SPACE system is based on a dynamic concept of simulating the production process of composite materials, i.e., in case of concrete: mixing of aggregates and paste, or cement and water. The details of the generation system have been published by the authors elsewhere [2,3]. To be able to simulate effects such as clustering and to reach high volume densities, element motion and inter-element collision are modelled [17], leading to effective ingredient mixing. This stage is referred to as the *dynamic stage*.

The general simulation concept can be described as follows:

- Initially, a structured or random 3-D *dilute* distribution of elements with pre-defined shape and size distribution (such as the grading curve) is generated within the boundaries of a container. So far, only spherical particles can be conceived by SPACE. This stage can be similar to that of a random generator based system. Next, random linear and rotational velocity vectors are assigned to each element.
- The second step, the actual dynamic stage, is an iterative procedure where location and orientation of all elements are changed at each time step according to a Newtonian *motion model*. This motion model relates the element's linear and angular displacement to a set of conditions enforced on the element (e.g., gravity, friction, etc.). When elements meet during this time interval, a *contact model* defines the effect of contact on the motion/rotation update. Inter-particle influences – one of the requirements for achieving a more versatile system – are incorporated in the *contact model*. Additionally, electrical or chemical inter-particle forces may be added to the *motion model*. This will allow to more accurately adjust SPACE simulations to the particle aggregation conditions (i.e. flocculation) of the fresh cement paste. In the present concept, the use of this facility was considered to needless complicate matters, because no quantitative estimation of the ITZ thickness was pursued. The density can be varied during this stage by changing the size of the container (compacting the structure), or by applying a gravitational force.
- Finally, the iteration stops when certain conditions are reached, such as the relevant volume fraction of aggregate, or the required water to cement ratio.

The final distribution state can incorporate effects due to gravity and to inter-particle influences. Simple physical laws may be used to define the inter-particle relationships, by introducing parameters such as specific mass and energy dissipation. Maximum packing densities can easily be simulated by the SPACE system. Such densities are relevant for aggregate packing problems on engineering level, or for binder particle packing problems particularly at low water to cement ratios, appropriate for High Strength or High Performance Concrete systems.

It should be noted finally, that the dynamic stage is a built-in mechanism to achieve high densities that cannot be realised by static simulation systems. The dynamic stage is supposed to imitate, moreover, the production stage of the material. All forces added to the system can be manipulated, so that 'sticky' particle contacts during the production of the model material can also be simulated. *The dynamic (Newtonian) simulation mechanism has no significance after completion of the simulation, hence, is not connected with the rheological properties of the model material.* Once mixed, the aggregated particles constitute a static system. This is the starting point for applying the hydration algorithm to the fresh cement paste.

2.3. Hydration process

The hydration process will be outlined in two steps. First, the representation of a hydrating cement particle as a set of concentric spheres will be clarified based on the hydration description of a single particle. This description largely follows the hydration description presented by van Breugel in [18]. Second, the more complicated situation of multiple merging particles will be evaluated.

2.4. Hydration of a single cement particle

The kinetic hydration process of a single particle consists of two subsequent stages in time. The first stage, in which a phase-boundary mechanism controls the hydration rate, is followed by a stage in which the reaction rate is controlled by a diffusion mechanism. The transition between the two stages is assumed to occur when the thickness of the layer of the reaction product $\mathrm{d}(t)$, precipitated on the cement particle at time t, equals a transition thickness δ_{tr}. The inward growth or decrease of the unhydrated cement surface Δr_{in} for a sufficiently small time period Δt is then given by

$$\Delta r_{\mathrm{in}} = \Delta t K_0 \left(\left(\frac{\delta_{\mathrm{tr}}}{\mathrm{d}(t)} \right)^{\beta} \right)^{\gamma} \tag{1}$$

where K_0 is the rate constant, $\gamma = 0$ as long as $\delta_{\mathrm{tr}} > \mathrm{d}(t)$ and $\gamma = 1$ otherwise. The constant β regulates the diffusion process. The chemical reaction between cement and water results in a gel-product. The relationship between the volume change ΔV_{in} of the hydrated cement and the volume change ΔV_{out} of the gel or outer product is given by

$$\Delta V_{\mathrm{out}} = v \Delta V_{\mathrm{in}} \tag{2}$$

with constant $v = 2.2$ [18]. A volume of ΔV_{in} of the reaction product is used to fill the space of the reacted cement. The remaining volume precipitates equally on the existing gel surface of the particle thereby introducing an outward growth. In this simulation the water will appear in three forms, i.e. chemical water, which is chemically bound to the cement by the hydration reaction, physical water which is adsorbed in the pores of the gel, and free water which is supposed to be the only form available for hydration. At initiation all water is free. An amount of water of 25% of the weight of the cement is chemically bound, and an amount of 15% by weight is physically bound. Consequently, a reacted volume of V_{in} cement requires a volume of water equal to

$$\Delta V_{\mathrm{fw}} = 0.4 \rho_{\mathrm{c}} \Delta V_{\mathrm{in}} \tag{3}$$

Herein $\rho_{\mathrm{c}} = 3.1$ (g/cm^3) represents the volumetric density of cement. Since the volume of the reaction product is smaller than the total volume of reacted cement and water, a fourth phase is introduced, air. Again, the reduction of the water supply occurs on the surface of the air–water interface, causing an outward growth of the air layer. The deposition of the gel product, and the consumption of cement and free water is assumed to be equally divided over the entire surface. Thus the cement-gel interface as well as the gel–air and air–water interfaces remain located on concentric spheres throughout the hydration process (see Fig. 1(a)). This is particularly convenient for modeling purposes. The product thickness $\mathrm{d}(t)$ in Eq. (1) is thus given by $r_{\mathrm{out}} - r_{\mathrm{in}}$. It should be noted that the formation of an air layer around the gel in the model is merely used to accommodate for the local consumption of water. It is not intended to represent the actual location of air. It is assumed that if water is still available (i.e. there exists an air–water interface) it will be equally available for the entire cement surface, hence causing a concentric decrease of the cement core. Note that at $t = 0$, $r_{\mathrm{in}} = r_{\mathrm{out}} = r_{\mathrm{fw}}$, and at $t > 0$, $r_{\mathrm{in}} \leqslant r_{\mathrm{out}} \leqslant r_{\mathrm{fw}}$. In brief, Eq. (1) yields the decrement of r_{in} per time step Δt, whereupon new values of r_{out} and r_{fw} can be obtained using Eqs. (2) and (3). This rather simple model holds as long as particles do not make contact and water does not run out.

2.5. Hydration of multiple cement particles

However, the simultaneous expansion of other particles in the vicinity will have the following severe effects on the hydration behavior:

- growing contact areas between the gel products of neighbouring particles diminishes the surface area that is available for product deposition. Fig. 1(b) illustrates a two-dimensional representation of this situation, whereby the thick line at the gel-air interface represents the free surface onto which the gel product may precipitate. Less surface area signifies a thicker deposit of the product layer.
- similarly, the consumption of water can only occur at the interface between air and free water (represented in Fig. 1(b) by the thick line at the air–water interface).
- the influences of contact on the inward growth of the cement is more complicated. A particle embedded in the gel layer, as illustrated in Fig. 1(b) - case *B*, prevents part of the gel surface to be active in the diffusion process. Moreover, the inward growth is also influenced by the reduction of free water (Fig. 1(b) - case *C*).

Let A_{fw} be the surface area of a sphere with radius r_{fw}, then $\omega_3 A_{\mathrm{fw}}$ corresponds to the total air–water surface and $\omega_2 A_{\mathrm{out}}$ equals the total gel-air surface. The factor ω_1 corresponds to the fraction of the total surface area that is active in the hydration process. The shielding effect as

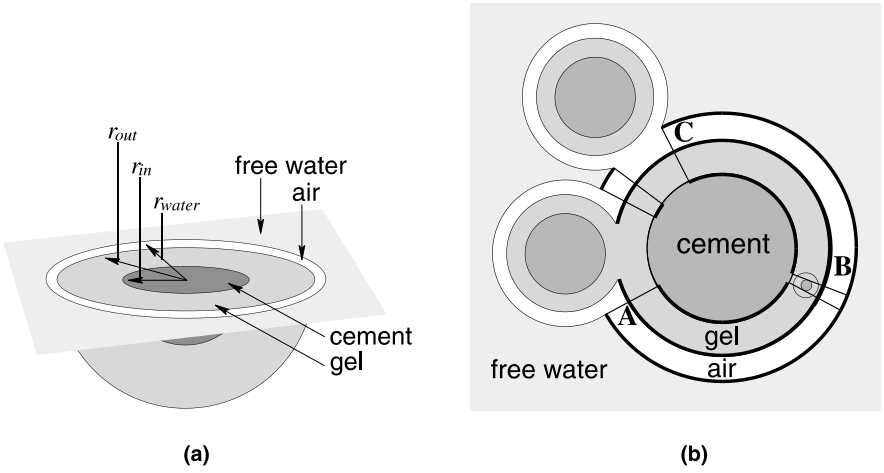

Fig. 1. (a) Geometrical representation of hydrated cement and (b) various contact situations between cement particles.

well as the water reduction are accounted for in ω_1. In the next section the values of ω_1, ω_2 and ω_3 will be evaluated.

2.6. Surface tesselation

To efficiently evaluate the free surface of a sphere an algorithm has been implemented that divides the surface in triangular tesserae, or surface patches as show in Fig. 2. By using an algorithm that generates a pentakisdodecahedron [19] of order k, the surface will be divided into $N = 2 \times 4^k$ surface patches of which only the centres are stored. It should be mentioned that the location of a specific point only changes in radial direction when the size of the sphere is altered. The fraction of the total spherical surface of the object that is not contained by any other object can now simply be determined by

$$\omega = \frac{n}{N} \tag{4}$$

in which n corresponds to N minus the number of patch centers that are contained by an arbitrary other sphere. As an example Fig. 2 shows the circular intersections of a sphere with two other (fused) spheres and the 10 detected surface patches that are contained by these spheres. The correction factor ω_3 of an object can now be obtained by counting the number of free surface patches n_3 when the size of each particle is temporarily changed to the radius of its own free water intersection (r_{fw}). Substitution of n_3 into Eq. (4) yields the required correction factor. The same calculation, but now with the size altered to r_{out}, yields the correction factor ω_2. The correction factor ω_1 is determined in two steps. First, the total number of sphere patches N that are active in the diffusion process is reduced by n_3 to accommodate for the water reduction (cases A and C of Fig. 1(b)). Second, it is checked whether the corresponding point on the gel-air surface of each remaining free surface point had been inactive during an earlier hydration stage. If so, they are considered inactive too. This operation imitates the shielding effect of particles that are partly embedded in the gel (case B of Fig. 1(b)). To conclude, an iterative repetition of the following procedure implements the hydration process

1. Determine Δr_{in} according to Eq. (1). Calculate the volume change ΔV_{in} when only a fraction ω_1 of the cement surface hydrates. Calculate a new value for the inward growth $\Delta r'_{\mathrm{in}}$ when a concentric decrease is assumed.
2. Determine ΔV_{out} using Eq. (2) and calculate the outward growth when precipitation only occurs on a fraction ω_2 of the surface A_{out}
3. Determine ΔV_{fw} using the relationship in Eq. (3) and calculate Δr_{fw} when water is only consumed from the surface area $\omega_3 A_{\mathrm{air}}$.

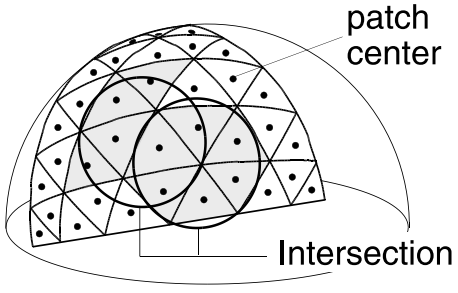

Fig. 2. Partly tesselated sphere surface. Grey area denotes the detected surface that is contained by one of the two spheres of which only the circular intersections are shown.

3. Cement particle packing at interfaces in fresh state

The density of mono-size particle packings is at higher volume fractions known to show a long-range

fluctuating behaviour as function of the distance to the interface. 'Long range' means that the effect of the interface will extend inward over several particle diameters. This case of which experimental data are available has been accurately simulated by SPACE, as a partial validation of the system [3]. A static sequential algorithm cannot accomplish this. For multi-size dense model cement particle packings, this phenomenon may be still of some relevance, as suggested by the present authors [13]. However, a possible long-range fluctuating behaviour of the larger particles is camouflaged in the present set up by the normal variation due to the limited number of particles. Hence, this would require an additional study.

A structure-sensitive property like crack initiation would basically appeal more to material configuration than to composition [1]. So, we have to deal in that case with a relatively bulky ITZ. This is due to the phenomenon of size segregation visualised in Fig. 3, and reproduced from an earlier publication of the authors [13]. For demonstration purposes, separate size fractions are studied of which the average size is basically stepwise increased by a factor 2. They demonstrate size segregation to occur. The particle size distribution function (i.e. particle grading) will therefore change as a function of the distance to the interface. This is shown in [20]. The gradient in pdf is extending relatively deep into the paste. As a consequence, the thickness of the ITZ shell will be considerably smaller when derived from density gradients than from configuration gradients, confirming experimental observations by Diamond and Huang [7].

By adding the density curves of the various particle fractions in Fig. 3, the global volumetric density versus distance to the interface curve is obtained. The part close to the interface reveals a steep and almost linear increase, characteristics for which the smaller particles in the (blended) model cement should receive credit. The second part of the curve is a transfer stage to a constant bulk value, obtained at a fraction, say one-third, of the maximum grain size away from the interface. Part of this transfer curve cannot easily be distinguished from bulk value, a problem also inherent to estimating the ITZ thickness from experimental measurements of gradient structure. Hence, the total fractional volume density curve seemingly reveals a less extended ITZ. However, the prime purpose of this discussion is not to estimate the ITZ's thickness accurately, but to demonstrate that the thickness depends on the evaluation parameter selected (in the range from composition to configuration); an evaluation parameter that is considered relevant for the mechanical property of interest (in the range from structure-sensitive to structure-insensitive properties). 'Hardness' or Young's modulus can be seen as examples of quite structure-insensitive properties [1]. The extent of the ITZ for such mechanical parameters will depend on particle density (volume fraction, water to cement ratio), and basically not on the details of the particle size distribution function.

Next, a parameter for evaluating the spatial structure of the particle packing in the ITZ is selected in the range between composition and configuration. It allows *demonstrating* the increased thickness of the related ITZ as compared to that for composition. For this demonstration purposes, the mean free path λ in μm is chosen. This parameter, that can be determined unambiguously in sections parallel to the interface surface, was earlier used for this purpose in [13]. The mean free path is the average of all *unobstructed* surface-to-surface distances to neighbouring particles [21]. As compared to the nearest neighbour distance, the mean free path has a reduced configuration-sensitivity, so its effect on the ITZ's thickness would certainly be not the most pronounced.

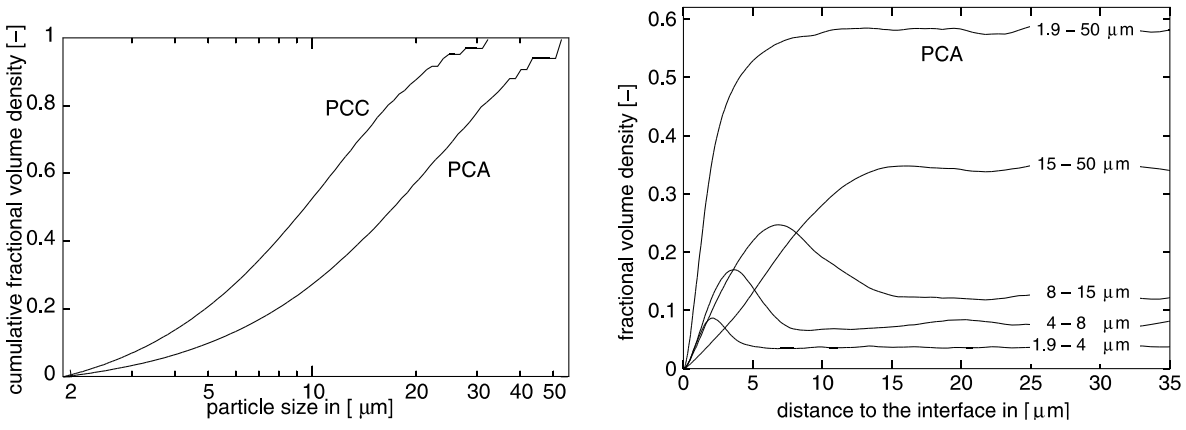

Fig. 3. Volumetric density of different size fractions of particles from model cement PCA, plotted as function of the distance to the interface (right); data are the average of six simulations based on the relevant particle size distribution function, pdf (left). These pdf's are at the basis of the simulations of Figs. 3–9.

It has been experimentally demonstrated that the addition to cementitious materials of fine mineral admixtures, whether pozzolanic or inert (like carbon black), contributed quite similarly to the strength of young concretes when having the same fineness [6]. Physical inter-particle bonding forces, therefore, should have their share in building up 'strength' of particulate materials like cementitious ones. Of course, it is not our aim to discuss such a concept in full depth. It is only mentioned to allow interpretation of the mean free path in a simple mechanical concept. For that purpose, the inter-particle bonding forces between close neighbours in the model cement particle packing of the young concrete are assumed Van der Waals type. Hence, a 'global bond strength' could be conceived proportional to λ^{-3} [22]. Although this *global* bond strength is not extremely structure-sensitive, the structural effects will be shown quite dramatic. It would permit to qualitatively assess the disproportional contributions of cement blending by fine mineral admixture as silica fume to 'improving the quality of the ITZ'.

3.1. Composition gradient in the ITZ

Figs. 4 and 5 present examples based on computer-simulations of cement pastes containing model cements with different Blaine numbers, i.e. PCA: 1760 cm^2/g, and PCC: 2660 cm^2/g, respectively. Model cements with a particle range of 1.9 to 50 μm are considered. Note that the Blaine numbers are relatively low, because of the cut off limit in the lower size range. The size range is limited because of computational reasons. *This does not fundamentally change the size segregation phenomenon revealed by Fig. 3, of course*. The particle size distribution function (pdf) of the model cements is made to closely match the Rosin–Rammler curve, $G(d) = 1 - \exp(-bd^n), n$ and b being constants with values $n = 1.3$, $b = 0.0175$ for PCA, and $n = 1.4$, $b = 0.033$ for PCC [3,18]. These pdf's are also presented in Fig. 3. The Rosin–Rammler curve is generally accepted to represent the particle size distribution of ordinary Portland cements. The well-established *Hymostruc* system [18] for simulation of hydration and structure formation is based on a similar concept (same pdf of spherical particles).

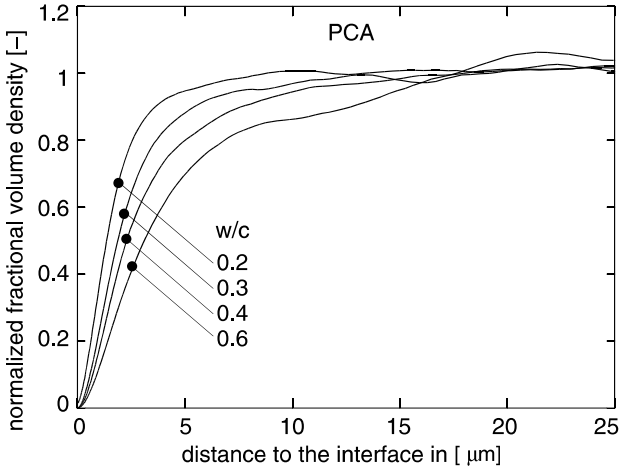

Fig. 4. Effect of water to cement ratio of the model cement paste (PCA) on volume density of the paste as function of the distance to the interface. The average results of six simulations are normalised by the bulk value of volume density.

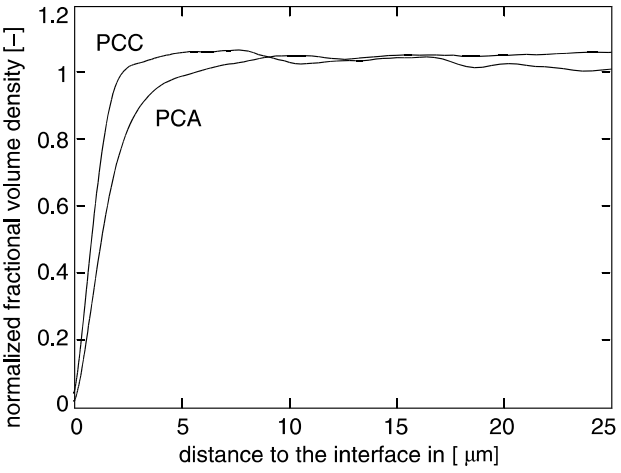

Fig. 5. Effect of the fineness of the model cement paste (PCA versus PCC) on the volume density gradient over the ITZ. The average results of six simulations are normalised by the respective bulk values of volume density.

Volume fraction of particles in the ITZ is analysed for step-wise reduced water to cement ratios in the range from 0.6 to 0.2. To do so, a total of 10 000 spherical grains were dispersed in a cubic container of which the size was gradually reduced to minimum linear dimensions of about 100 μm. The bulk value of volume fraction is used to normalise the data. This total number of grains ensures that the number of larger particles in the model cement is so large that the actual pdf does not seriously deviate from the continuous Rosin–Rammler function, as demonstrated by Fig. 3 (left). Increasing the maximum grain size would require to proportionally increase the container size. This would have a third power effect on the total number of particles. Despite economic algorithms in SPACE that avoid considering the position of all particles in studying the 'neighbourhood' of an arbitrary particle, this would have a very significant effect on computer time. *Note that all data represent the average of six simulations.* Results are obtained by an *automated analysis of serial sections* parallel to the interface surface, discussed later. Stereological interpretation yields the 3-D density information plotted as function of the distance to the interface.

Fig. 4 demonstrates the ITZ's thickness in the lower range of water to cement ratios (0.2–0.4) to be in the order of 1/3rd of maximum grain size. The parameter at issue is the local value of particle volume fraction normalised by its bulk value. This is a composition criterion. Thickness of the ITZ is increased over the full range of water to cement ratios by a factor of about 2 [3]. More accurate estimates could be obtained by increasing the number of simulations and averaging the data, but main purpose here is to reveal *trends*. Fig. 5 reveals the change in ITZ thickness due to cement fineness (1760 and 2660 cm^2/g) for a paste with a W/C ratio of 0.2. Data are normalised by the respective bulk values of volume fraction. Additionally, porosity (interpreted here as complementary to particle volume density) declines significantly faster away from the interface in case of the finer cement. It can be expected that the addition of fine mineral admixtures such as silica fume will significantly enhance this rate in porosity decline in the vicinity of the interface.

3.2. Configuration gradient in the ITZ

Figs. 6–9 deal with effects of water to cement ratio and fineness of the binder on the global bond strength. The same PCA and PCC as defined in Fig. 3 are employed for this purpose. Figs. 6 and 7 show the effect of the reduced water to cement ratio on the bond capacity of the model cement paste containing the coarser cement type (PCA). Fig. 7 presents the data normalised by the relevant bulk values. Hence, sufficiently far away from the interface the ordinate value is 1 (apart from statistical variation). With a reduction in W/C ratio, the inter-particle bond capacity more steeply rises in the immediate vicinity of the interface to a level that at lower water to cement ratios even exceeds bulk value. Hence, also the bond between the cement particles and the aggregate surface will increase proportionally. At increasing distance to the interface, unit value is gradually approached. The disproportional improvement of bond in the part of the ITZ immediately neighbouring the interface surface is restricted to the range of W/C = 0.2 to 0.3 (relevant for HPC). This is accompanied by a significant increase in the ITZ thickness.

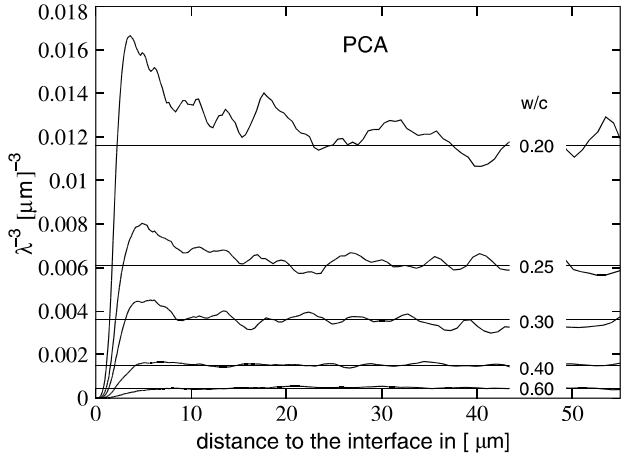

Fig. 6. Parameter proportional to global bond capacity in the ITZ as function of the water to cement ratio (PCA); λ = mean free spacing in μm. The average results of six simulations are presented.

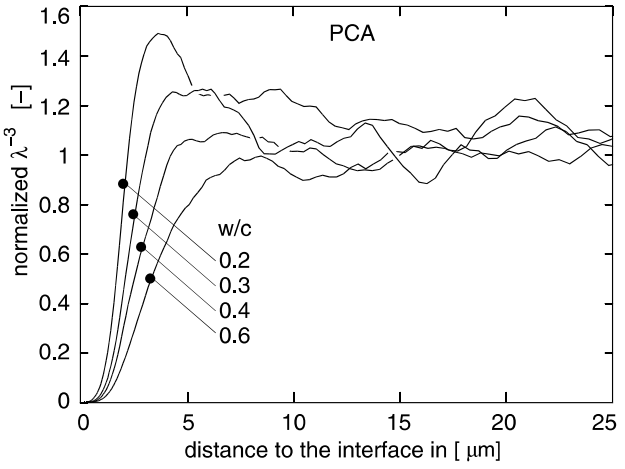

Fig. 7. Data of Fig. 6 normalised by the respective bulk ordinate values. λ = mean free spacing in μm. The average results of six simulations are presented.

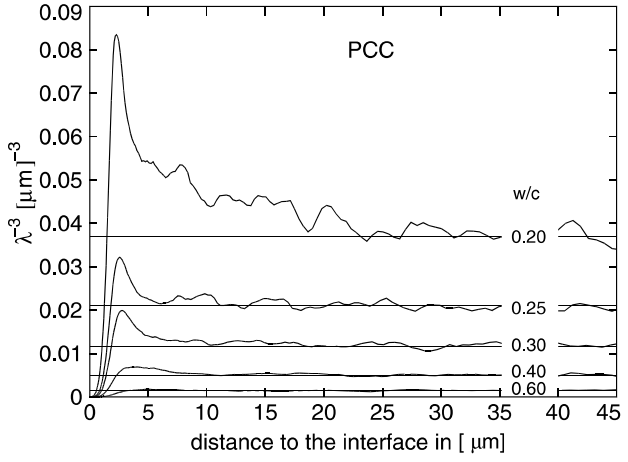

Fig. 8. Parameter proportional to global bond capacity in the ITZ as function of the water to cement ratio (PCC); λ = mean free spacing in μm. The average results of six simulations are presented.

Fig. 8 deals with the fine-grained cement. The disproportional bond strength increase in the ITZ neighbouring the interface becomes already apparent at W/C = 0.4. The strength increase is more dramatic than in case of the coarser model cement (PCA). The latter effect is clearly revealed by Fig. 9 that presents the global bond

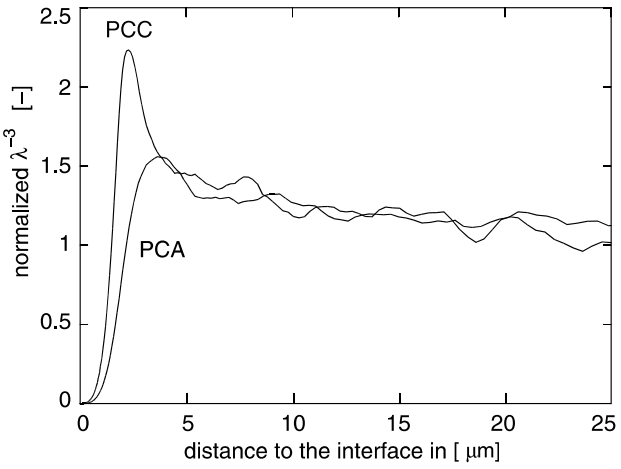

Fig. 9. Normalised global bond capacity data of Figs. 6 and 8 for W/C = 0.2 as function of the distance to the interface.

capacity data normalised by the relevant bulk values. Data are pertaining to the two model cements used in pastes with a water to cement ratio of 0.2. Size segregation causes an accumulation of the smaller particles close to the interface (as demonstrated in Fig. 3). This gives rise to a more rapid growth in inter-particle bond to a level that is 2.25 times exceeding the bulk property. This is about 40% exceeding the peak bond level of the PCA paste. Hence, selecting a fine-grained cement (larger Blaine number) or adding a mineral admixture with particles smaller than those of the cement (silica fume) will lead to a similar size-segregation phenomenon and a further disproportional improved bond capacity. A comparison between Figs. 6 and 8 learns the average level of the plotted parameter (which is supposed to be proportional to a global bond capacity) to be in all cases on a significantly higher level for the fine-grained model cement (PCC). The ITZ thickness increases with reduced water to cement ratios and is of the order of maximum grain size in the model cement for W/C = 0.2. Hence, the extent of the ITZ depends on the composition of the material (W/C ratio) and on the position of the measuring parameter in the range between composition and configuration. The latter conclusion can be derived from a comparison of similar cases (e.g. PCA, W/C = 0.2) in Figs. 4 and 6.

Note that the centre of the smallest particles in the mixtures will be at least at a distance of 1 μm from the interface. Maximum bond capacity of the finest cement (PCC) is attained at a distance of about 2.5 μm. In case of the second cement (PCA), this is about 4 μm. Hence, the building up of maximum bond capacity takes place over distances of approximately 1.5 μm for PCC and 3.0 μm for PCA, respectively; a difference of 100%. Since inter-particle distances in the layer immediately bordering the interface will be similar to particle-interface distances, the same conclusion can be drawn as to the level of physical bond between the particles and the interface surface.

Although not primarily targeted in this paper, it would be of interest to see whether the gap can be bridged between experimental data and the presented simulation results on model cements. The SPACE system allows to assign forces to the particles in the dynamic stage of the simulation process to more closely simulate aggregation mechanisms, such as flocculation. In the future also particle shape could be remodelled, although computational efforts for 'contact detection' will increase significantly. But, of course, simulating material structure inevitably asks for making structural simplifications. Nevertheless, the detection of trends in the aggregation of particular matter can be accomplished in a relatively easy way, whereby outcomes can be checked by comparison with actual measurements. The SPACE system provides a couple of additional parameters (like internal energy dissipation during the dynamic stage) which influence the aggregation process. For examples, see [3]. This would allow narrowing the gap between a real material and a model 'material' in a specific situation.

In comparing ITZ measurements on real materials and simulation data, we should account for the larger size range of real cements. This will exert a direct effect on the ITZ's extent (see, e.g. Fig. 3). For the sake of the argument, proportionality is therefore assumed between the ITZ's thickness and the maximum grain size. For a cement with a noticeable fraction of grains in the 80 to 100 μm size range, this would lead to a roughly 20–25 μm thick ITZ shell for composition, and an 80 to 100 μm one for configuration. Of course, water to cement ratio and fineness of the binder will influence these data in a moderate way for composition measurements, and strongly for configuration parameters, as demonstrated herein. In comparing with experimental data we have to acknowledge that experimental data on the ITZ's thickness may reflect other mechanisms than 'packing', although a common one as interface bleeding is probably of minor importance in the HPC range. Finally, experimental observations cannot easily be obtained on ITZ sections perpendicular to the aggregate grain's surface, leading to biased information. Even averaging over a series of random observations on apparent ITZ sections in a single large-scale section of the specimen would lead to estimates about 50% too large [11]. A general but fundamental problem is that the ITZ has no clear and obvious boundaries. Determination of the ITZ's thickness from gradient measurements, either experimental or simulated ones, can therefore neither be very accurate nor completely objective. Of more importance is therefore the recognition that the extent of the ITZ, though hard to delineate, will depend on material composition, as well as on the degree of depen-

dence of the parameter being studied on material configuration. The assessment of this phenomenon was the prime purpose of this paper.

3.3. Cement packing at interfaces in hardened state

An interesting field for application of computer-simulation systems is cement hydration. To allow for realistic explorations of the structural implications of the hardening phenomenon, 'hydration' has been implemented in SPACE. As to the validity of the approach, reference can be made to a close correspondence found between the measured strength development of hydrating cement pastes by Locher [23] and SPACE simulations for pastes with three different water to cement ratios (*i.e.* W/C = 0.26, 0.388 and 0.50), assuming the strength development to be proportional to the growing contact surface area per unit of volume [3].

Preliminary results [3,24] obtained by way of SPACE simulations revealed maturity to have opposite effects on normal concretes and on HPCs; at low water to cement ratios, the ITZ thickness declined somewhat with maturity, whereas an increase was detected for normal concrete (W/C>0.42) [3]. However, the gradient pattern of the particle packing stage is not changing *fundamentally*, as can be seen also in Fig. 10. The effect of water to cement ratio on configuration is significant, as we have seen before. This leads during hardening to dramatic effects. By reducing the water to cement ratio from 0.5 to 0.4, image patterns made at 10 years hardening revealed a connected pore structure (Fig. 10) to transforms into a disconnected network in bulk of the model material [3,25]. A further reduction in the water to cement ratio from 0.4 to 0.26 yielded the number and total volume of anhydrous cement to increase disproportional. In both cases, the distributions of pore clusters and of anhydrous cement particles showed a large degree of inhomogeneity. This conforms to experimental observations published in the literature [7,8,12]. The explanation is the configuration-sensitivity of both phenomena. The higher porosity in the ITZ causes a significant reduction in the anhydrous cement content, but the gradient will still be governed by configuration. Hence, the ITZ's thickness based on the anhydrous cement content homogeneity will exceed the one for composition considerably. This is also confirmed by Diamond and Huang [7].

3.4. Automated section analysis

The quantitative structural analysis of the ITZ requires sampling in *sections parallel to the interface*. Experimentally, this would require a laborious process of physical sectioning and quantitative image analysis by point or line scanning operations. Instead, conventionally, narrow strips are subjected to image analysis procedures. These strips run parallel to the interface, but are situated in the very section in which the gradient structure is investigated. These image analysis processes can be automated, of course. A pre-requisite is in many cases that the quality (contrast) in the image is enhanced by subjecting it to pattern recognition algorithms. This inevitably leads to extra scatter and even biases. In the present situation of *model cements*, the spatial distribution of all particles is known (with respect to the coordinates and associated radius of each particle), so structural 3-*D* information attributed in the SPACE system to a section does not suffer from such inevitable experimental 'uncertainties'.

A relevant 2-D parameter reflecting the composition gradient is the areal fraction of the particles, A_A. By taking a full section of 100×100 μm^2, the areal fraction can be determined accurately. A_A is an unbiased estimator of V_V, the volume fraction of particles, either of a

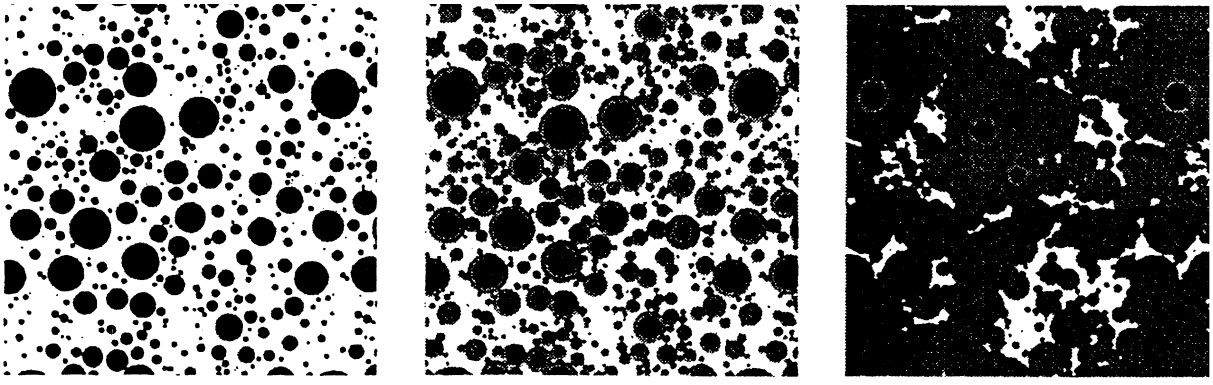

Fig. 10. Sections of bulk cement paste with W/C = 0.5 during hydration; (a) initial stage, (b) after 3.2 days, and (c) after 10 years of hydration (white areas indicate water/air, grey areas represent gel and black areas correspond to unhydrated cement).

narrow range of particle sizes (as accomplished for Fig. 3), or for the full size range of particles.

The mean free path is linked to 3-D structural information accessible in a section, i.e. $\lambda = 4(1 - V_V)/S_V$, whereby S_V is the specific surface area of the particles. The total perimeter length of the circular cross-sections of the particles per unit of area in the section plane, L_A, is related to the surface area per unit of volume by $S_V = \frac{4}{\pi} L_A$. This allows for an unbiased and exact estimation of λ. The mean free spacing was employed earlier by Stroeven for the *experimental* assessment of particle packing characteristics in concrete [26].

4. Conclusions

Computer-simulation can establish the details of the packing phenomenon at aggregate grain interfaces of model cements. The SPACE system allows to influence the packing phenomenon by incorporating forces in the dynamic simulation stage. This makes the system versatile. The effects of implemented mechanisms should be validated by experiments, of course. Since this paper aimed at revealing *trends in the packing phenomenon*, these complications were avoided. Limited validation has been accomplished earlier (e.g. mono-size particle packings compacted to maximum fractional density, and strength development during hydration of model cement pastes). This demonstrated the system to be at least reliable in a qualitative respect.

SPACE simulations on model cements clearly revealed the trends in changing water to cement ratio and cement fineness on volume fraction of cement particle gradients in the ITZ. The thickness of the ITZ was in all cases a portion of the maximum grain size of the model cement. The investigated volume fraction parameter measures *composition* of the simulated cement structure in the ITZ.

By separating the model cement particles in successive size ranges, SPACE demonstrated the occurrence of size-segregation in the ITZ, i.e. the finer the particles, the closer the peak value of the volume fraction of such particles is situated with respect to the interface. Particle grading fluctuations extent much deeper into the material body than those of the composition parameter, total volume fraction. Hence, the associated ITZ would have a larger thickness. Grading of particles governs size and spacing of the particles, so is a *configuration* parameter.

The paper introduces an average bonding capacity related to the reciprocal value to the third power of the mean free spacing (i.e. λ^{-3}). This is a structural parameter in the range between composition and configuration (i.e. of medium configuration-sensitivity). The more dramatic effects due to changes in W/C ratio, and cement fineness on the gradient in this parameter inside the ITZ are presented. Particularly under conditions relevant for HPC (W/C = 0.2, finest cement), the ITZ is significantly densified and thus the 'bonding capacity' *disproportional improved*. The associated ITZ would have a thickness of the order of maximum grain size of the cement.

The *ITZ has no distinct boundaries* due to the gradual transfer to bulk features. Deriving the thickness of the ITZ for a given composition and for the associated parameter of interest from gradient structural information would be equally difficult for experimental and simulated data.

References

[1] Freudenthal AM. The Inelastic Behavior of Engineering Materials and Structures. New York: Wiley; 1950.

[2] Stroeven M, Stroeven P. Computer-simulated internal structure of materials. Acta Stereol 1996;15(3):247–52.

[3] Stroeven M. Discrete numerical model for the structure assessment of composite materials, PhD thesis. Delft, Delft University of Technology;1999.

[4] Jiang W, Roy DM. Strengthening mechanisms of high-performance concrete. In: Malhotra VM, editor. High Performance Concrete, Proceedings ACI International Conference Singapore. Detroit: ACI. 1994, p. 753–67.

[5] Fidjestøl P, Frearson J. High performance concrete using blended and triple blended cements. In: Malhotra VM, editor. High Performance Concrete, Proceedings ACI International Conference Singapore. Detroit: ACI. 1994, p. 135–57.

[6] Detwiler RJ, Metha PK. Chemical and physical effects of silica fume on mechanical behaviour of concrete. ACI Mat J 1989;86(6):609–14.

[7] Diamond S, Huang J. The interfacial transition zone: reality or myth? In: Katz A, Bentur A, Alexander M, Arlinguie G, editors. The Interfacial Transition Zone in Cementitious Composites. London: E and FN Spon. 1998, p. 3–39.

[8] Ollivier JP, Maso JC, Bourdette B. Interfacial transition zone in concrete. Adv Cem Bas Mat 1995;(2):30–38.

[9] Wang Y. The effect of bond characteristics between steel slag fine aggregate and cement paste on mechanical properties of concrete and mortar. In: Mindess S, Shah SP, editors. Bonding in Cementitious Composites, MRS Symp Proc 114, 1988;49–54.

[10] Holliday L. Geometrical considerations and phase relationships. In: Holliday L, editor. Composite Materials. Amsterdam: Elsevier; 1966. p. 1–27.

[11] Stroeven P. Analytical and computer-simulation approaches to the extent of the interfacial transition zone in concrete. In: Brandt AM, Li VC, Marschall IH, editors. Proceedings Brittle Matrix Conference 6 Cambridge. Woodhead and Z Turek RSI. 2000, p. 465–74.

[12] Scrivener, KL. The microstructure of concrete. In: Skalny JP. editor. Materials Science of Concrete I. Westerville (OH), Am Ceram Soc 1989;127–61.

[13] Stroeven P, Stroeven M. Micromechanical behaviour of concrete interpreted by computer simulation system for material structure. In: Carlomagno GM, Brebbia CA, editors. Computational Methods and Experimental Measurements IX. Southampton: WIT Press; 1999. p. 571–82.

[14] Roelfstra PE. A numerical approach to investigate the properties of numerical concrete. PhD thesis. Lausanne;EPFL-Lausanne:1989.

[15] Diekkämper R. Ein Verfahren zur numerischen Simulation des Bruch- und Verformungsverhaltens spröder Werkstoffe. Techn Wissenschaftliche Mitteilungen der Institut für Konstruktiven Ingenieursbau, Ruhr Universität Bochum, 1984 (7).
[16] Bentz DP, Garboczi, EJ, Stutzman PE. Computer modelling of the interfacial zone in concrete. In: Maso JC, editor. Interfaces in Cementitious Composites. London: E and FN Spon. 1993, p. 107–16.
[17] Brach RM. Mechanical Impact Dynamics, Rigid Body Collisions. New York: Wiley; 1991.
[18] Breugel K van. Simulation of hydration and formation of structure in hardening cement-based materials. PhD thesis, Delft, Delft University of Technology, 1991.
[19] Silla E, Tuñón I, Pascual–Ahuir JL. GEPOL: An improved description of molecular surfaces II computing the molecular area and volume. J Comp Chem 1991;12(9):1077–88.
[20] Stroeven P, Stroeven M. SPACE simulation of particle packing in the ITZ; a spatial perspective on the ITZ's relevance. In: Proceedings International Symposium High Performance Concrete – Workability, Strength and Durability, Hongkong and Shenzhen, 10–15 December 2000 (to be published).
[21] Fullman RL. Measurement of particle sizes in opaque bodies. Trans Met Soc AIME 1953;197(March):447–52.
[22] Wittmann F. Experiments to determine Van der Waals forces. In: Te'eni M, editor. Structure, Solid Mechanics and Engineering Design. London: Wiley-Interscience; 1971. p. 295–300.
[23] Locher FW. Die Festigkeit des Zements. Beton 1976;26(8):283–5.
[24] Stroeven M, Stroeven P. Simulation of Hydration and the Formation of Microstructure. In: Owen DRJ, Oñate E, Hinton E, editors. Computational Plasticity. Barcelona: CIMNE; 1997. p. 981–7.
[25] Navi P, Pignat C. Simulation of cement hydration and connectivity of the capillary pore space. Adv Cem Bas Mat 1996;(4):58–67.
[26] Stroeven P. Some Aspects of the Micromechanics of Concrete. PhD thesis, Delft, Delft University of Technology, 1973.